THE CANADIAN MINERALOGIST
Journal of the Mineralogical Association of Canada

Volume 19 November 1981 Part 4

Canadian Mineralogist
Vol. 19, pp. 505-518 (1981)

SELECTED-AREA ELECTRON-CHANNELING PATTERNS FROM GEOLOGICAL MATERIALS: SPECIMEN PREPARATION, INDEXING AND REPRESENTATION OF PATTERNS AND APPLICATIONS

G.E. LLOYD AND M.G. HALL
Centre for Materials Science, University of Birmingham, Birmingham B15 2TT, Great Britain

B. COCKAYNE
Royal Signals and Radar Establishment, Malvern, Worcestershire WR14 3PS, Great Britain

D.W. JONES
Centre for Materials Science, University of Birmingham, Birmingham B15 2TT, Great Britain

ABSTRACT

Selected-area electron-channeling patterns (SAECP) obtained in scanning electron microscopy can be used to accurately determine the crystallographic orientation of individual mineral grains. This paper describes a technique for producing SAECPs from a grain size of $\geqslant$ 1 μm. It involves the use of back-scattered electrons and a new specimen-polishing method which, while producing very flat surfaces, does so without introducing significant mechanical damage. Methods of indexing and representing the patterns are also described, including the use of spherical SAECP maps and the construction of pole figure, inverse pole figure and orientation-distribution-function diagrams. Finally, two examples are given of the applicability of SAECPs to petrofabric and deformation–fracture studies.

Keywords: scanning electron microscopy, electron channeling, crystallographic orientation, petrofabric analysis, deformation.

SOMMAIRE

Les clichés de canalisation d'électrons obtenus sur une région restreinte par microscopie électronique à balayage peuvent servir à déterminer l'orientation cristallographique précise de grains individuels de minéraux. On décrit ici une technique permettant d'obtenir de tels clichés sur des cristaux d'une taille $\geqslant$ 1 μm; cette technique utilise les électrons rétrodiffusés et une nouvelle méthode de polissage qui donne une surface très plane sans dommage mécanique appréciable. L'indexation et la représentation des clichés, notamment par projection sphérique, par construction de figures de pôle, de figures de pôle inversées et de diagrammes de la fonction de distribution de l'orientation, sont discutées. Deux exemples illustrent l'application de tels clichés à l'analyse de la pétrofabrique et à l'étude de fractures dues à la déformation.

(Traduit par la Rédaction)

Mots-clés: microscopie électronique à balayage, canalisation d'électrons, orientation cristallographique, analyse de la pétrofabrique, déformation.

INTRODUCTION

The determination of the crystallographic orientation of individual grains or of the overall fabric of a polygranular specimen is of considerable interest to geologists. Traditional geological methods have relied on optical microscopy (*e.g.*, Emmons 1943), but X-ray-diffraction techniques have also become important over the last two decades (*e.g.*, Starkey 1964, Baker

et al. 1969, Phillips & Bradshaw 1970). However, both approaches have disadvantages. Optical methods are laborious and are restricted to a few specific orientations and minerals, but they do permit the simultaneous consideration of other specimen characteristics. X-ray techniques are indiscriminate with regard to individual grains and therefore do not permit the simultaneous consideration of other characteristics, but most minerals and orientations can be analyzed. In this contribution we discuss a method of determining crystallographic orientation using the scanning electron microscope (SEM) that enables individual grains in bulk specimens to be oriented while simultaneously allowing other characteristics (*e.g.*, grain size, shape, dimensional orientation, structure and composition) to be considered.

There are currently three techniques available for determining the crystallographic orientation of solid samples in the SEM. These are Kossel X-ray diffraction (*e.g.*, Dingley & Biggin 1973), electron back-scattering patterns (*e.g.*, Venables & Harland 1973) and selected-area electron-channeling patterns. The first two techniques are not employed very often, possibly because of problems associated with their use. For example, Kossel X-ray diffraction is restricted to a narrow range of atomic numbers (approximately $Z = 19$ to 30) and requires the insertion of photographic film inside the SEM; electron back-scattering patterns also require considerable instrumental modification. Selected-area electron-channeling patterns (SAECPs), on the other hand, require fewer instrumental modifications, are applicable to all atomic numbers and, once obtained, may be used to measure orientations rapidly and easily.

SAECPs were first observed by Coates (1967) and interpreted by Booker *et al.* (1967) in terms of the theoretical models for orientation dependence of X-ray emission discussed earlier by Hirsch *et al.* (1962). They arise from the "channeling" of the primary electron beam by the crystallographic lattice of the specimen and consist of lines and bands, the appearance of which is unique for a particular orientation; see reviews by Joy (1974) and Schulson (1977). The patterns have been used by metallurgists to study crystallographic orientation, recrystallization, deformation (including plasticity, crystal defects and fracture), grain-boundary structure and radiation damage in metals and alloys; a bibliography has been compiled by Joy & Newbury (1977). Saimoto *et al.* (1980) have shown that it is possible to obtain some form of SAECP from geological materials, although their examples are of poor quality. Prior to their study, the use of SAECPs by geologists was limited because of problems associated with specimen preparation. This contribution describes several alternative techniques to those used by Saimoto *et al.* that result in patterns of considerably superior quality and discusses how the patterns may be used in the study of some geological problems. For a comprehensive discussion of the many aspects of scanning electron microscopy and electron channeling, the reader is referred to Goldstein & Yakowitz (1975).

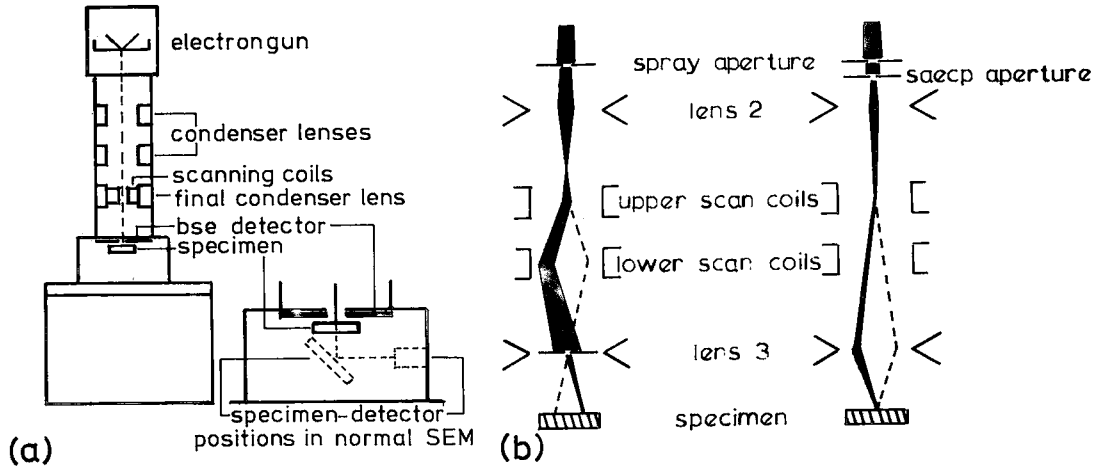

FIG. 1.(a) General configuration of the SEM (Cambridge Stereoscan 4) showing the positions of specimen, electron beam and backscattered electron detector. (b) Schematic ray diagrams for SEM operation in micrographic mode (left) and SAECP mode (right); see also Hall & Hutchinson (1980).

SEM Configuration

The configuration of our SEM (Cambridge Stereoscan 4) for the production of SAECPs is shown in Figure 1a; note especially the relative positions of the primary electron-beam, back-scattered-electron (BSE) detector and specimen. This arrangement differs from that used by Saimoto *et al.* (1980), who employed the absorbed specimen-current for imaging and a shorter working distance ($\sim$ 1 mm) rather than the BSEs. We find that the use of BSEs and a suitable detector inserted between the final lens plate of the SEM and the specimen greatly improves image detail, mainly by increasing the proportion of the total signal due to electron channeling. This approach also reduces the risk of artifacts, such as specimen charging and

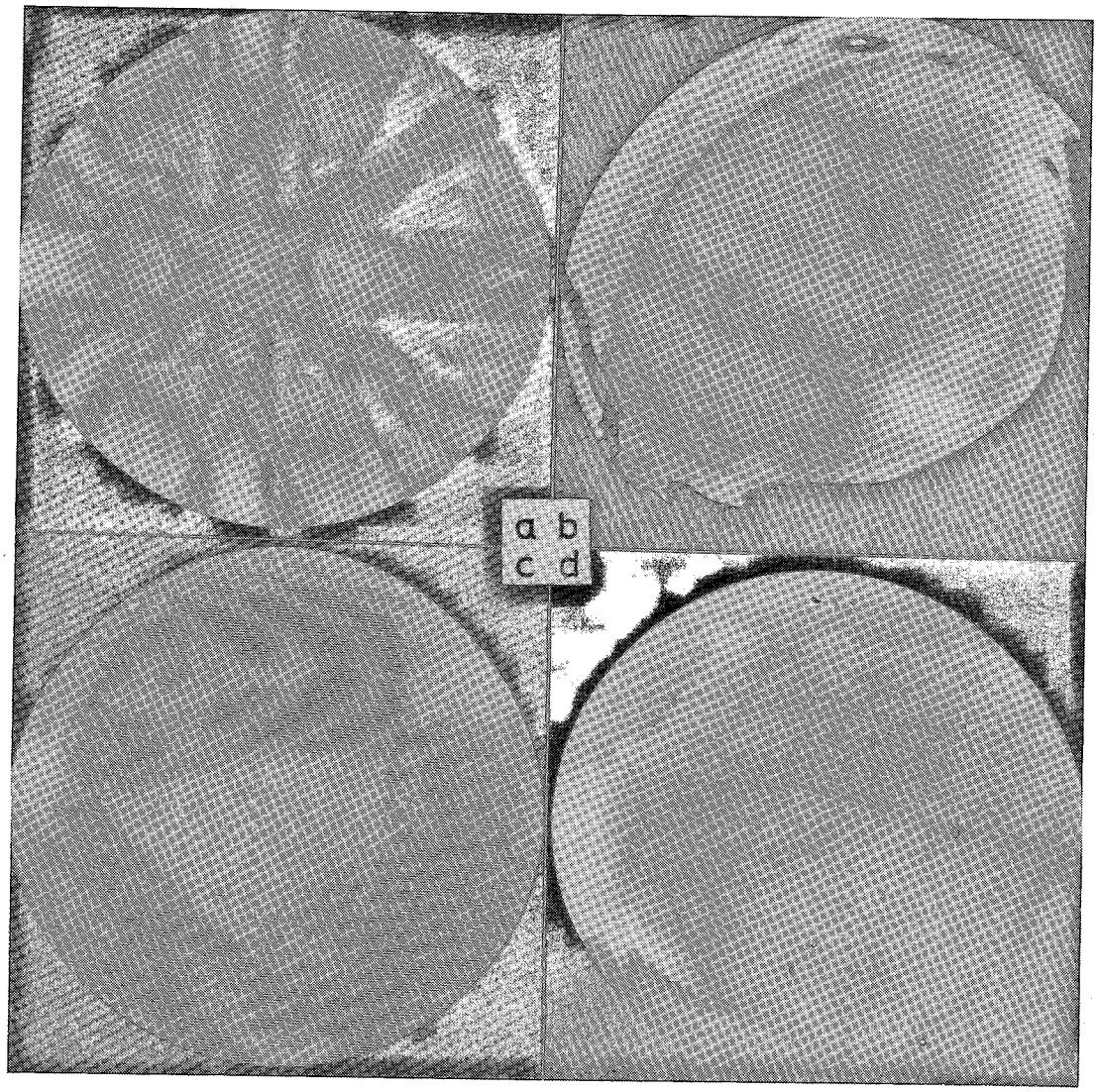

FIG. 2. Examples of SAECPs from variously prepared specimen surfaces: (a) electro-polished surface of copper (face-centred cubic symmetry), (b) vibratory polished surface of synthetic rutile (tetragonal symmetry), (c) natural cleavage surface of synthetic periclase (cubic symmetry), (d) natural crystal face of quartz (rhombohedral symmetry). Accelerating voltage is 30 kV in all cases; all except (a) carbon coated.

contamination caused by the primary beam. Several BSE detector systems are available (*e.g.*, Wolf & Everhart 1969, Robinson 1975); ours consists of a single annular *p–n* silicon diode (Stephen *et al.* 1975), although we have also used silicon photodiodes with comparable results (Hall & Lloyd 1981). In both cases, we used a specimen working distance of 5–10 mm (resulting in less beam convergence than for a 1 mm working distance) and an accelerating voltage of 30 kV.

To obtain SAECPs, the primary electron beam has to be "rocked" about a point on the specimen surface rather than scanned over an area. This can be achieved in several ways, for instance, by the addition of an extra set of scanning coils (the "after-lens deflection" method of Schulson 1971b) or by using the final condenser lens to bring the electron beam to a point on the sample, usually by switching off one set of scan coils of the double deflection scanning system (the "deflection focusing" method of van Essen *et al.* 1971). We use the latter method (as detailed in Fig. 1b) which, in a SEM, is capable of rocking the beam about a minimum dimension of $\sim$ 10 μm. However, this can be reduced to 1–2 μm by dynamic focusing of the final lens (van Essen 1971, Hall & Skinner 1978).

Only a small proportion ($\sim$ 5%) of the total BSE signal is caused by electron channeling; most is due to multiple scattering. It is therefore necessary to provide a large amount of "black level" to make the contrast visible (Newbury 1975). The intensity of the BSE current depends on the angle of incidence between the primary beam and the specimen's crystallographic lattice; rocking the beam causes this angle to vary and results in differences in the intensity. SEM images produced by this method show the variation in channeling intensity with angle of incidence (Fig. 2a) and are known as SAECPs. Because they result from the specific relationship between primary beam and a specimen's crystallographic lattice, SAECPs are unique for a particular crystallographic orientation; provided specimens are suitably prepared, they can be used to accurately determine the crystallographic orientation of bulk specimens.

Specimen Preparation

SAECPs have been obtained from pure metals and alloys (*e.g.*, Coates 1967, Joy 1974, Schulson 1977); it is well known that the quality of pattern is adversely affected by specimen deformation, such that for strains > 8–10% only diffuse patterns are formed (*e.g.*, Stickler *et al.* 1971, Spencer *et al.* 1974). Specimens must therefore have constant lattice orientation over the region about which the beam is rocked (*i.e.*, a minimum dimension of 10–15 μm for a deflection-focusing system or 1–2 μm if dynamic focusing is used). It is also essential for specimens to be flat; surface topographic effects will tend to overwhelm the small proportion of the total signal due to electron channeling. Consequently, considerable specimen preparation is necessary. However, conventional grinding and polishing with diamond abrasive pastes usually cause sufficient deformation in the specimen to destroy any channeling effects, which originate from no deeper than the first 500 Å of the surface. Possibly for this reason, the production of SAECPs from geological materials has, until recently, been limited. For example, the quartz single crystal used in Figure 3 showed only very diffuse and unrecognizable SAECPs when it was diamond-polished but excellent quality patterns when prepared using the technique described below.

Saimoto *et al.* (1980) have obtained SAECPs of variable clarity from several geological specimens, and we have obtained images of similar or superior quality (*e.g.*, Fig. 2b) using vibratory polishing. However, for reasons we shall discuss later, in most cases these SAECPs do not contain sufficient detail to be of use in petrofabric analysis. In the rest of this section, we describe a specimen-preparation technique that usually gives superior results. Although natural surfaces (*e.g.*, crystal or cleavage faces) sometimes produce SAECPs without any preparation (*e.g.*, Fig. 2c, d), this is restricted to large grained specimens or single crystals.

The specimen-preparation technique employs procedures that have been developed for polishing mechanically hard single-crystal materials (*e.g.*, refractory oxides) widely used in laser, electro-optic and surface acoustic-wave devices (Fynn & Powell 1979). Samples are wax-mounted on metal plates and attached to a standard optical polishing jig, where they are ground to uniform flatness using 600-grade carborundum grit on a smooth cast-iron lap. The next stage involves polishing the samples on a spiral-grooved pitch lap with a paste of Linde 0.3A alumina diol as the abrasive. This stage is done using a standard machine in which the lap rotates in a horizontal plane and the jig holding the specimen is reciprocated in a fixed line along 80% of a lap radius. The final polish is obtained on a polyurethane pad using an

alkali silica sol slurry (Syton®, Monsanto Chemical Corporation, London, England) as the polishing agent, the slurry being recirculated continually over the rotating lap. To ensure damage-free surfaces, samples are thoroughly cleaned between each polishing stage to prevent coarse particles (of both abrasive and specimen) from being carried forward to produce damage during later polishing. The cleaning is a progressive process using water throughout and involving mechanical scrubbing with a soft brush followed by high-pressure washing and completed by ultrasonic rinsing. For further details, especially of the types of wax and lubricants available, see Fynn & Powell (1979).

The size of specimen that can be polished varies considerably; for example, the pyrite specimen considered below is 4 x 3 x 1 cm thick, whereas the quartzite specimen is 1.5 x 1.5 x 0.3 cm thick; both larger and smaller specimens can be accommodated. The maximum size is probably ultimately determined by the dimensions of the SEM specimen chamber. The duration of polishing depends on the specimen

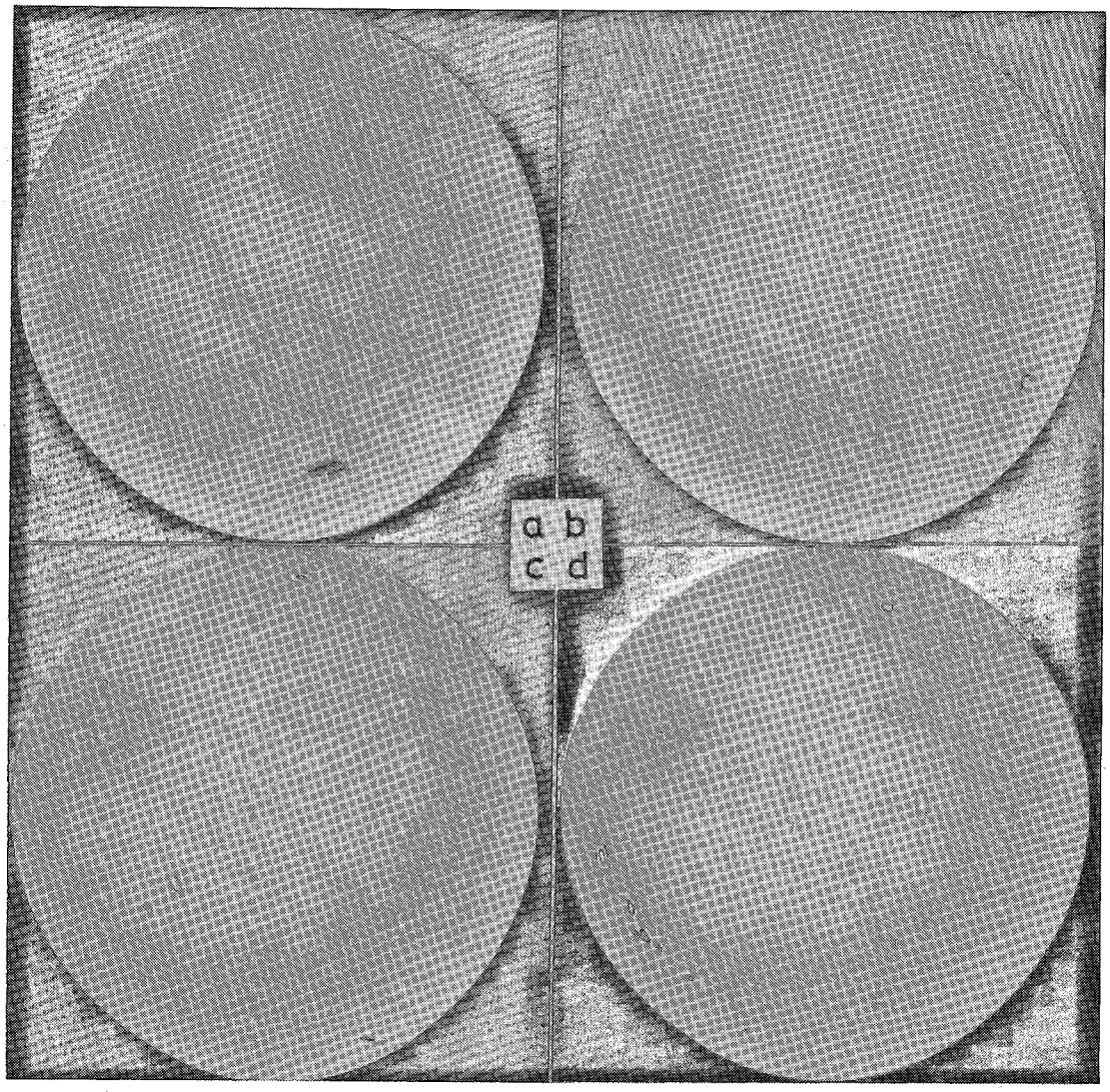

FIG. 3. Effect of increasing thickness of surface film (carbon) on SAECP quality. (a) 70 Å thickness, (b) 120 Å, (c)) 180 Å and (d) 220 Å. Natural quartz single crystal; 30 kV.

and can be only a few minutes for soft specimens but several hours for hard ones. The pressure applied to the specimen also determines, to some extent, how long the polishing takes; however, too much pressure can lead to tearing of the specimen surface.

As with other polishing techniques, polyphase specimens, especially those with considerable contrasts in hardness, do present some difficulties. Nevertheless, with care it is possible to polish such specimens adequately (for example, the pyrite specimen considered below consists of broken fragments of pyrite in a mainly calcite matrix, which represents a considerable difference in relative hardness). However, the initial stages of polishing prior to the use of Syton assume importance since the production of smooth surfaces with no topographic features, such as at phase boundaries, is essential for equilibrium Syton polishing. Impregnated specimens may also be polished without fear of break-up.

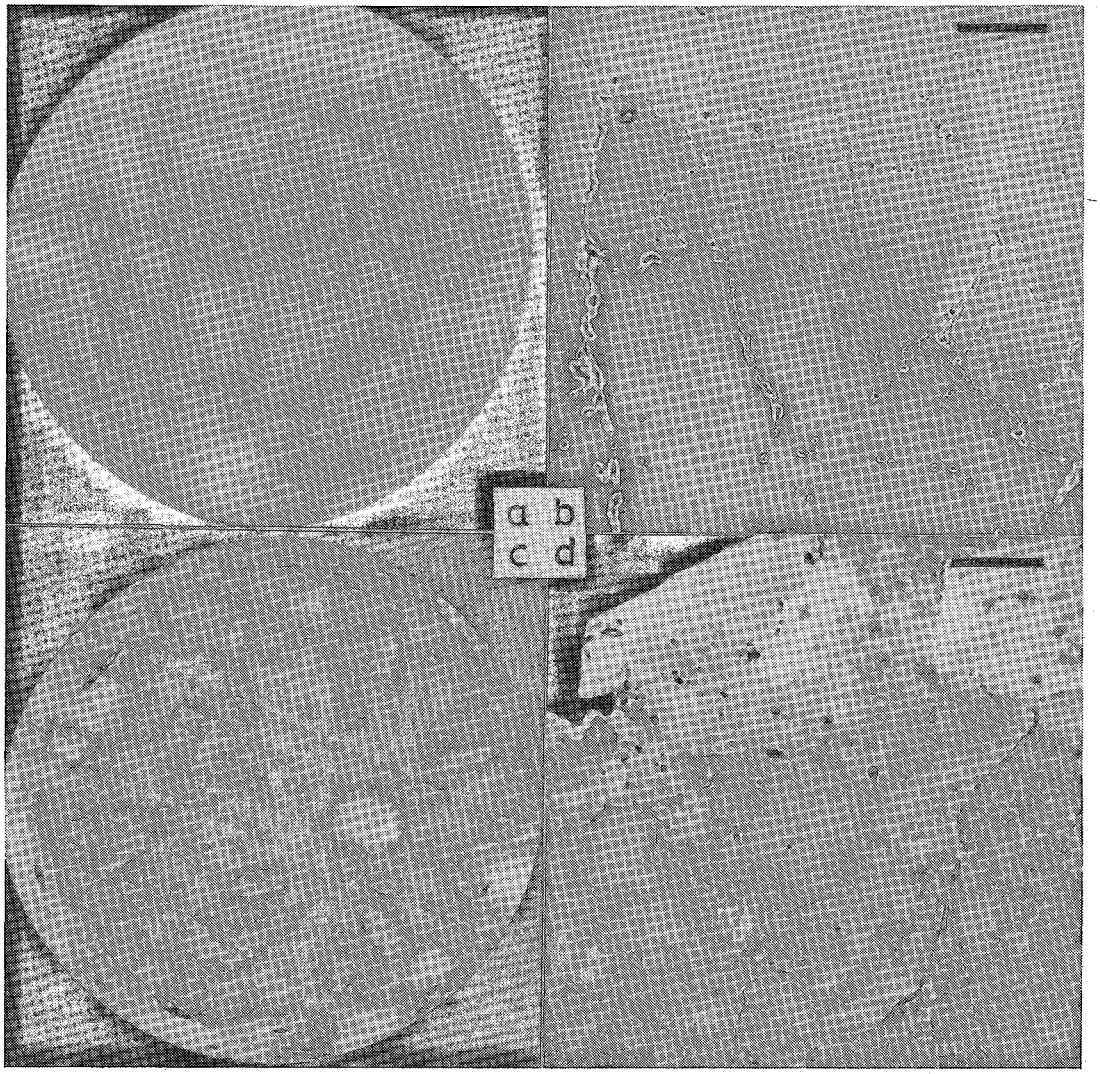

FIG. 4. Examples of SAECPs from rocks: (a) quartzite, $(2\bar{1}\bar{1}0)$ orientation, (b) electron-channeling contrast image of quartzite; scale bar 50 μm, (c) pyrite, (114) orientation, (d) electron-channeling contrast image of pyrite; scale bar 100 μm. All examples 30 kV; (a) and (b) carbon coated.

After polishing, it is usually necessary to coat a geological specimen with a thin layer of conducting material to prevent the specimen from charging under the influence of the primary electron beam. However, because electron-channeling effects originate from only the first few hundred Ångstrom units of the specimen, as the thickness of the conducting layer increases, the detail in the SAECP decreases. This effect is illustrated in Figure 3, using a natural single crystal of quartz polished according to the above method and coated with carbon. The carbon is deposited by vacuum evaporation, and the thickness is controlled by using a commercial quartz crystal monitor (Edwards High Vacuum Ltd. FTM 2). We find that $\sim$ 70 Å of carbon is usually sufficient to prevent specimen charging but still allows good quality SAECPs to be obtained (Fig. 3a). Some geological specimens (*e.g.*, metal sulfides) do not re-

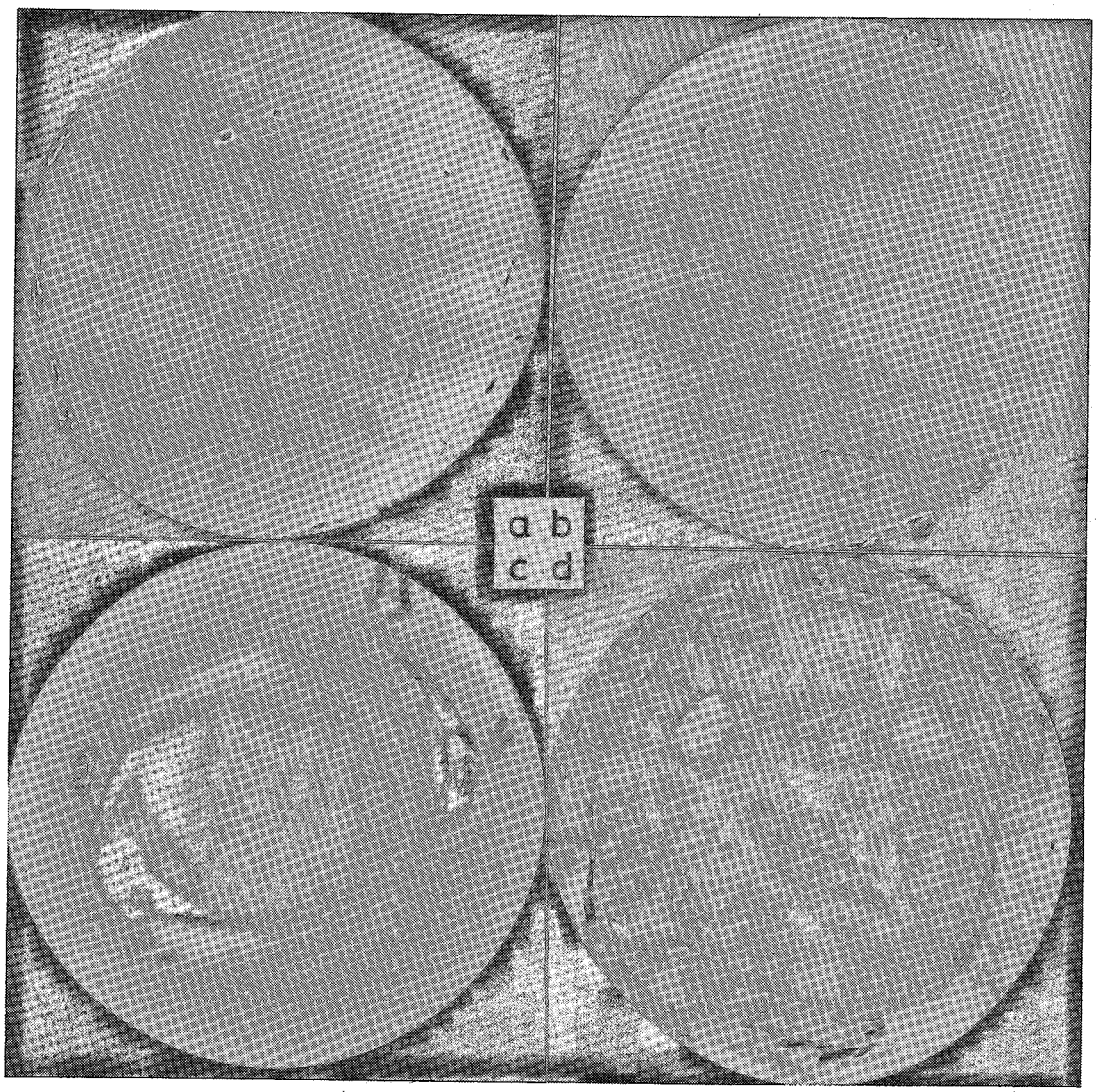

FIG. 5. Examples of SAECPs to be expected: (a) major crystallographic orientation (pole), quartzite; (1$\bar{1}$00) orientation; (b) no major crystallographic orientation, quartzite; (c) interference from surface film (carbon), single crystal of natural quartz; (d) interference from adjacent SAECPs, pyrite. All examples 30 kV; all except (d) carbon coated.

quire coating as they are sufficiently conductive to dissipate a charge.

SAECPs from Geological Specimens

In addition to the examples illustrated (Figs. 2, 3), we have obtained SAECPs from grains in quartzite and pyrite (Fig. 4). It is known, however, that certain materials (*e.g.*, the alkali halides) decompose under the beam and locally lose their crystallinity (Schulson 1971a). Saimoto *et al.* (1980) reported this behavior for calcite; it is possible that other minerals also will degrade in the SEM.

Figure 4 also shows the grain structures from which the patterns originate. These images are produced by orientation contrast, a mechanism related to that which gives rise to SAECPs, obtained when the primary beam is scanned over an area rather than rocked about a point. The contrast is caused by differences in electron channeling from each grain that reflect differences in orientation. Orientation contrast can therefore be used to determine grain size, shape and dimensional orientation as well as any intragrain features and is especialy useful when used in combination with SAECPs.

Indexing of SAECPs

For easy indexing, SAECPs must be of good quality. In particular, the high index lines must be clearly visible. This is especially important for those patterns that do not consist of prominent crystallographic features or "poles" (for example, compare Figs. 5a, b), or those that cover only a small proportion of the total image, because of either the size of the specimen region considered (Fig. 5c) or general interference from surrounding regions (Fig. 5d). In all cases, clear, sharp patterns are essential for accurate indexing. The simplest method of indexing a SAECP is to compare it with a "SAECP map" (Joy 1974). Such maps (*e.g.*, Fig. 6) consist of all the individual SAECPs required by symmetry to cover the crystallographic stereogram or unit triangle sufficiently to represent all orientations. The maps are constructed by tilting a single grain (or crystal) of the material to different orientations about a fixed point of incidence of the primary beam. In principle each mineral requires its own SAECP map, but in practice it is often sufficient to use a map of the same crystallographic symmetry. As the symmetry decreases,

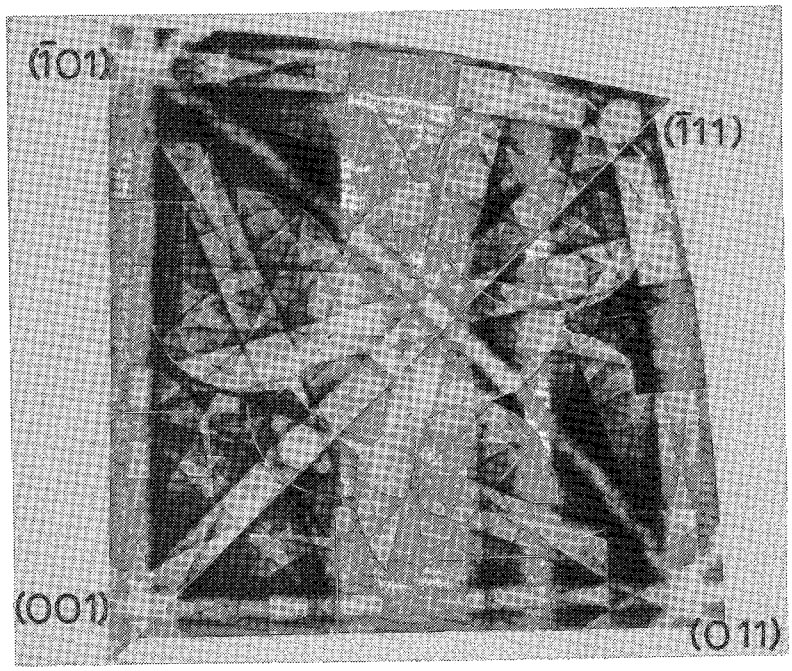

FIG. 6. SAECP map for face-centred materials of cubic symmetry. The map actually covers two stereographic unit triangles and was constructed from a copper single-crystal sphere; 30 kV.

the area of the stereogram increases; consequently, so does the size of the SAECP map, resulting in distortion of the patterns and causing problems in fitting together the component SAECPs. These difficulties may be overcome by the use of a sphere (Stott *et al.* 1975) or several smaller maps (*e.g.*, Fig. 7) centred on major orientations (Joy 1974).

Alternative methods of indexing SAECPs involve computer-generated maps (*e.g.*, Young & Lytton 1972, 1977, K.M. Knowles, pers. comm. 1979) and analytical examination of the patterns. In the latter method the relationship between the spacing of pairs of lines in the SAECP and the Miller indices is used to determine the orientation (Joy 1974).

Use of SAECPs

SAECPs have been used in metallurgy to study crystallographic orientation, recrystallization, deformation, fracture, grain-boundary structures and lattice-parameter determinations. Consequently, they should also be of considerable use in geology. In this section the use of SAECPs in fabric analysis (especially the development of fabric diagrams) and in deformation and fracture studies is discussed.

Fabric analysis

To determine the overall fabric of a specimen, it is necessary to consider collectively the orientations of a large number of grains. The conventional geological method of representing large numbers of orientations is by means of the pole figure or fabric diagram, in which a specific crystallographic direction (*e.g.*, the *c* axis) is plotted with respect to the specimen co-ordinate system on a stereographic projection. Pole figures are prepared directly from orientation data measured either optically or by X-ray diffraction. An alternative to the pole figure is the inverse pole figure or axis distribution chart, which represents the orientation of a specific fabric element in crystallographic co-ordinates. Inverse pole figures can be derived either from a function that represents a complete description of the crystal orientations in the specimen or from several measured pole figures for different orientations. However, both pole and inverse pole figures fail to give a complete description of the fabric, as they involve only two of the three degrees of freedom that all orientations possess. They are therefore merely projections of the three-dimensional orientation-distribution function (ODF), which is the complete fabric description.

Fig. 7. Partial SAECP map for quartz centred on $(1\bar{1}00)$. Carbon coated; 30 kV.

Methods for using pole or inverse pole figure data to determine ODFs involve the use of three angular measurements (Roe 1965, Williams 1968, Bunge 1969, Bunge & Wenk 1977). Two angles fix the position of the normal to the specimen plane with respect to the crystallographic axes; the third fixes the position of a chosen reference direction in the specimen plane with respect to the other two. For example, in slates it is usual to consider the foliation plane and a lineation direction within this plane, whereas metallurgists make frequent use of rolling plane and rolling direction in rolled specimens. ODFs can therefore be represented graphically by three orthogonal axes, with each orientation corresponding to a point in three-dimensional space, although for convenience they are usually depicted as a series of planar sections contoured to show the intensity of orientation development (*e.g.*, Hatherley & Hutchinson 1979).

We have seen that each SAECP is unique for

a particular orientation and that it can readily be indexed by comparison with the relevant SAECP map. The simplest method of representing a large number of patterns is to mark each position on an overlay of a SAECP map, which results in an inverse pole figure (Fig. 8a). This method is quick and accurate (to a few degrees) and can easily be adapted to give Miller

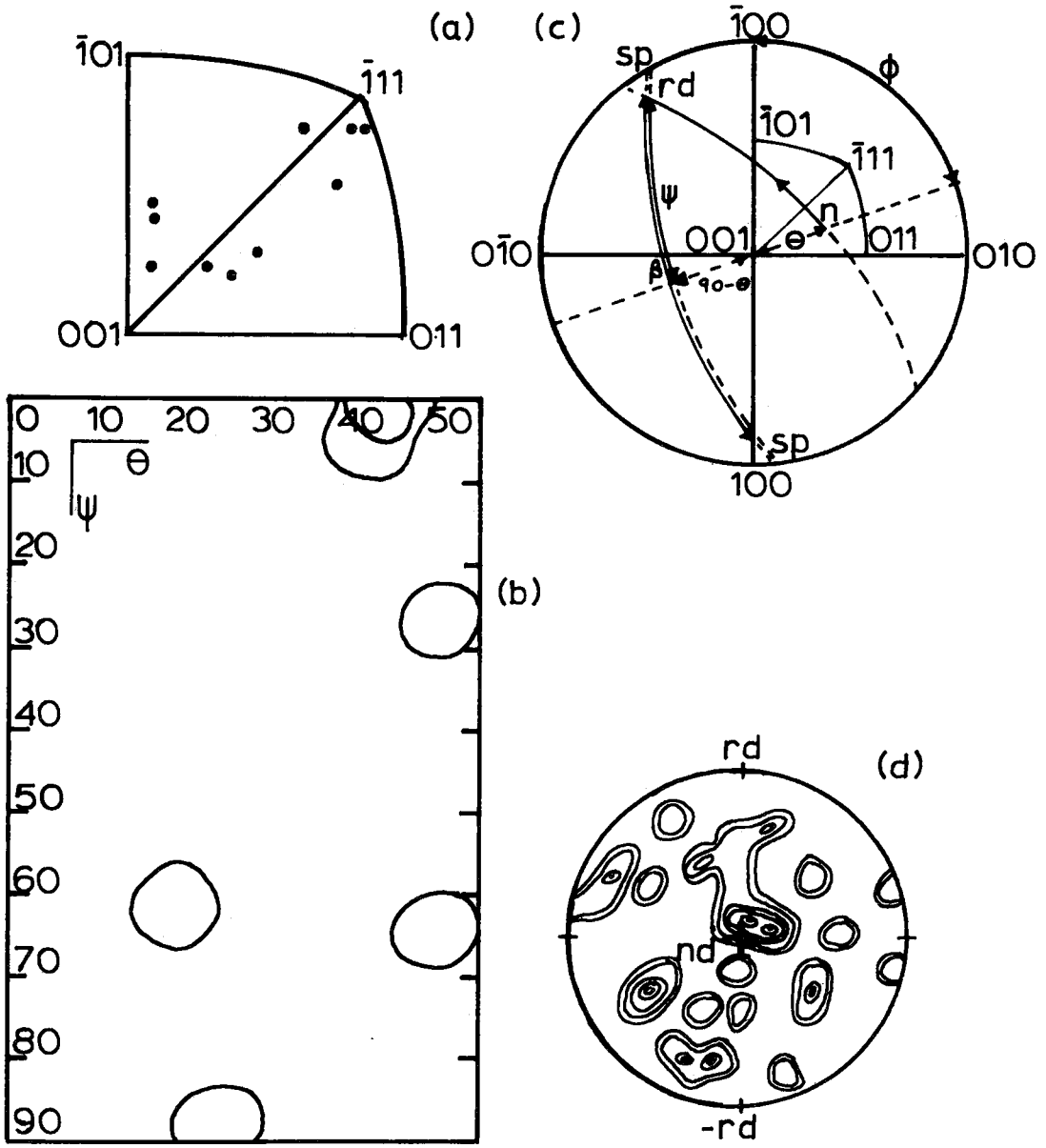

FIG. 8. Methods of representing large numbers of SAECPs for petrofabric analysis (all data from pyrite grains): (a) inverse pole figure, positions of SAECP/specimen normal marked on overlay of SAECP map; (b) orientation distribution function $\phi = 45°$ plane, contour intervals 1%; (c) determination of three Euler angles from SAECPs: sp specimen plane, rd reference direction in sp, n normal to sp (and SAECP; see text); (d) {001} pole figure: rd specimen reference direction, n normal to specimen plane.

indices (Joy 1974), but it fails to give a complete description of the orientation, as it does not consider rotation about the marked position. However, SAECPs can be used to construct ODF diagrams and hence give a complete description of the specimen (Fig. 8b); the following account describes how this is done for materials with cubic symmetry.

Each SAECP represents the specimen-normal position with respect to the crystal axes. This position is located by measuring two angular distances θ and ϕ (Fig. 8c). A third angle ψ is needed to fix the position of a chosen reference direction in the specimen plane with respect to the other two; this is determined by measuring the angle β and using the relationship $\psi = \beta - \tan^{-1/2}(\tan\phi\cos\theta)$ (see Williams 1968). The SAECP reference direction usually chosen is the vertical line across the pattern through the orientation, since this can be made to correspond to a chosen specimen-direction, although it is important that corrections are made

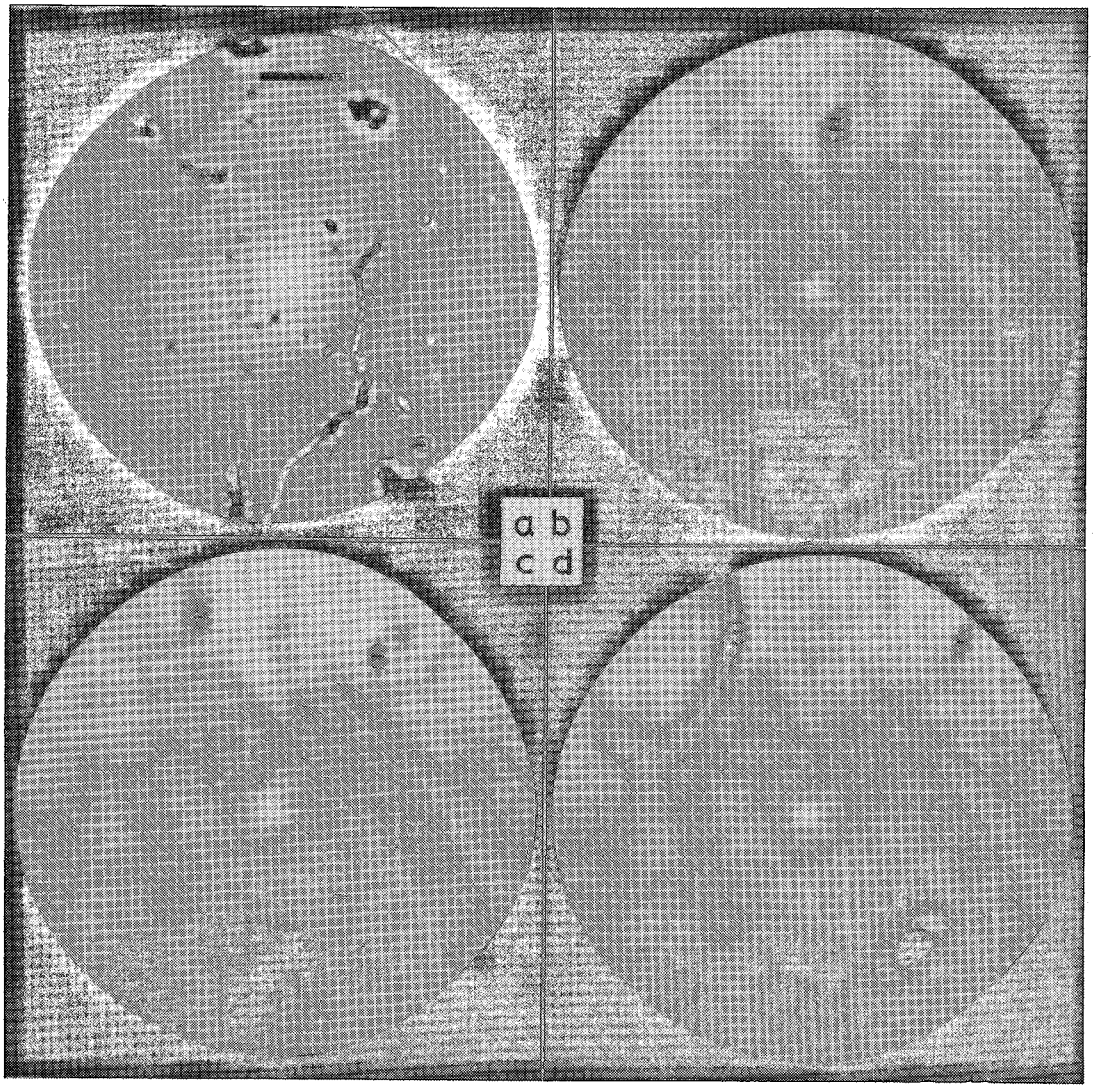

FIG. 9. Example of use of SAECPs in the study of deformation: (a) electron-channeling contrast image of intragranular crack in pyrite; scale bar 25 μm; (b) undistorted SAECP from region remote from crack; (c) and (d) distorted SAECPs from regions close to crack. All are carbon coated; 30 kV.

to allow for the rotation between SAECPs and ordinary SEM micrographs (*e.g.*, van Essen & Verhoeven 1974). A convenient way of measuring the three angles is to construct the SAECP map over the surface of a sphere and to use curved rulers graduated in degrees to measure the distances (Stott *et al.* 1975).

Williams (1968) has described a method for constructing pole figures from the Euler angles obtained from SAECPs (Fig. 8d). This is useful, since pole figures are more familiar to geologists than are ODF diagrams. However, it must be emphasized that only ODFs give a complete description of the fabric.

Deformation and fracture

The quality of SAECPs is ultimately determined by the state of the crystallographic lattice at the rocking position (Joy *et al.* 1972, Spencer *et al.* 1974); consequently, channeling patterns can be used in the study of (plastic) deformation (*e.g.*, Stickler *et al.* 1971). Although it may even be possible to obtain quantitative information regarding amounts of deformation (Davidson 1974), it is a simple matter to compare SAECPs from different grains and to relate changes in pattern quality to variations in amounts of deformation. As an example, we shall consider the pyrite discussed above.

The pyrite occurs in masses in a calcareous matrix and has suffered "chocolate-tablet" boudinage (D. Dietrich & J.G. Ramsay, pers. comm. 1980) with individual pyrite "boudins" partly traversed by intergranular or intragranular cracks (or both) (Fig. 9a). Good-quality SAECPs are obtained from regions remote from the cracks (Fig. 9b), but adjacent to the cracks the lines and bands become distorted (Figs. 9c, d), indicating a "crack-tip" region of plastic deformation. Such behavior has important consequences with regard to mechanisms of fracture (*e.g.*, Davidson *et al.* 1976, McMeeking 1977) and has recently been considered by Lloyd & Ferguson (1981) with regard to boudinage. SAECPs therefore have considerable potential in the study of rock deformation and fracture.

Summary

Selected-area electron-channeling patterns (SAECPs) produced in the scanning electron microscope (SEM) allow the accurate determination of the crystallographic orientation of geological materials. Provided careful specimen-preparation techniques are used, grains (or subgrains) as small as 1–2 μm can be indexed. Orientations determined from SAECPs can be represented in various forms, including orientation-distribution-function diagrams. Since each grain is imaged individually, it is therefore possible, using other SEM techniques such as atomic number contrast (*e.g.*, Hall & Lloyd 1981) and electron-channeling contrast, to consider simultaneously other aspects (*e.g.*, grain or subgrain size, shape, dimensional orientation and intergrain relationships). The incorporation of an X-ray analysis system also allows composition to be determined. The SEM is therefore potentially a very powerful instrument in contemporary geological research.

Acknowledgements

We thank Dr. W.B. Hutchinson for his comments on an earlier version of this manuscript and his continued interest. The pyrite specimen was obtained from Dr. D. Dietrich and Professor J.G. Ramsay; Dr. C.C. Ferguson provided the quartzite specimens.

References

Baker, D.W., Wenk, H.R. & Christie, J.M. (1969): X-ray analysis of preferred orientation in fine-grained quartz aggregate. *J. Geol.* **77**, 144-172.

Booker, G.R., Shaw, A.M.B., Whelan, M.J. & Hirsch, P.B. (1967): Some comments on the interpretation of the 'Kikuchi-like reflection patterns' observed by scanning electron microscopy. *Phil. Mag.* **16**, 1185-1191.

Bradshaw, R. & Phillips, F.C. (1970): The use of X-rays in petrofabric studies. *In* Experimental and Natural Rock Deformation (P. Paulitsch, ed.). Springer-Verlag, Berlin.

Bunge, H.J. (1969): *Mathematische Methoden der Texturanalyse.* Akademie-Verlag, Berlin.

——— & Wenk, H.R. (1977): Three-dimensional texture analysis of three quartzites (trigonal crystal and triclinic specimen symmetry). *Tectonophys.* **40**, 257-285.

Coates, D.G. (1967): Kikuchi-like reflection patterns obtained with the scanning electron microscope. *Phil. Mag.* **16**, 1179-1184.

Davidson, D.L. (1974): A method for quantifying electron channelling pattern degradation due to material deformation. *Proc. Seventh Ann. Scanning Electron Microscopy Symp.* IV, 927-934.

———, LANKFORD, J., YOKOBORI, T. & SATO, K. (1976): Fatigue crack-tip plastic zones in low carbon steel. *Int. J. Fract.* **12**, 579-585.

DINGLEY, D.J. & BIGGIN, S. (1973): A comparison of the Kossel X-ray diffraction technique with the electron channelling technique. *In* Scanning Electron Microscopy: Systems and Applications. Institute of Physics, London.

EMMONS, R.C. (1943): The universal stage. *Geol. Soc. Amer. Mem.* **8**.

FYNN, G.W. & POWELL, W.J.A. (1979): *The Cutting and Polishing of Electro-Optic Materials.* Adam Hilger Ltd., London.

GOLDSTEIN, J.I. & YAKOWITZ, H. (1975): *Practical Scanning Electron Microscopy*, Plenum, New York.

HALL, M.G. & HUTCHINSON, W.B. (1980): Smooth surface metallography using the scanning electron microscope. *The Metallurgist & Maters. Technologist* **12**, 371-375.

——— & LLOYD, G.E. (1981): The SEM examination of geological samples with a semiconductor back-scattered electron detector. *Amer. Mineral.* **66**, 362-368.

——— & SKINNER, G.K. (1978): A spiral scanning attachment for electron channelling studies with a scanning electron microscope. *J. Phys. E* **11**, 1129-1132.

HATHERLEY, M. & HUTCHINSON, W.B. (1979): An introduction to textures in metals. *Inst. Metall. (London) Mon.* **5**.

HIRSCH, P.B., HOWIE, A. & WHELAN, M.J. (1962): On the production of X-rays in thin metal foils. *Phil. Mag.* **7**, 2095-2100.

JOY, D.C. (1974): Electron channelling patterns in the scanning electron microscope. *In* Quantitative Scanning Electron Microscopy (D.B. Holt, M.D. Muir & P.R. Grant, eds.). Academic Press, New York.

——— & NEWBURY, D.E. (1977): A bibliography on the observation of crystalline materials by use of diffraction effects in the scanning electron microscope. *Proc. Tenth Ann. Scanning Electron Microscopy Symp.* I, 445-454.

———, ——— & HAZZLEDINE, P.M. (1972): Anomalous crystallographic contrast on rolled and annealed specimens. *Proc. Fifth Ann. Scanning Electron Microscopy Symp.* I, 97-104.

LLOYD, G.E. & FERGUSON, C.C. (1981): Boudinage structure: some new interpretations based on elastic–plastic finite element simulations. *J. Struct. Geol.* **3**, 117-128.

MCMEEKING, R.M. (1977): Finite deformation analysis of crack-tip opening in elastic–plastic materials and implications to fracture. *J. Mech. Phys. Solids* **25**, 357-381.

NEWBURY, D.E. (1975): Techniques of signal processing in the scanning electron microscope. *Proc. Eighth Ann. Scanning Electron Microscopy Symp.* I, 727-736.

OATLEY, C.W. (1972): *The Scanning Electron Microscope.* Cambridge University Press, Cambridge, England.

PRINCE, K.C. & MARTIN, J.W. (1979): The effects of dispersoids on the micromechanisms of crack propagation in Al–Mg–Si alloys. *Acta Metall.* **27**, 1401-1408.

ROBINSON, V.N.E. (1975): Backscattered electron imaging. *Proc. Eighth Ann. Scanning Electron Microscopy Symp.* I, 51-60.

ROE, R.-J. (1965): Descriptions of crystallite orientation in polycrystalline materials. III. General solution to pole figure inversion. *J. Appl. Phys.* **36**, 2024-2031.

SAIMOTO, S., HELMSTAEDT, H., KEMPSON, D. & SCHULSON, E.M. (1980): Electron channeling and its potential for petrofabric studies. *Can. Mineral.* **18**, 251-259.

SCHULSON, E.M. (1971a): A scanning electron microscope study of the degradation of electron channeling effects in alkali halide crystals during electron irradiation. *J. Mat. Sci.* **6**, 377-383.

——— (1971b): Generating electron channelling patterns in the JSM–II SEM. *J. Mat. Sci.* **6**, 447-448.

——— (1977): Electron channelling patterns in scanning electron microscopy. *J. Mat. Sci.* **12**, 1071-1087.

SPENCER, J.P., BOOKER, G.R., HUMPHREYS, C.J. & JOY, D.C. (1974): Electron channelling patterns from deformed crystals. *Proc. Seventh Ann. Scanning Electron Microscopy Symp.* I, 919-926.

STARKEY, J. (1964): An X-ray method for determining the orientation of selected crystal planes in polycrystalline aggregates. *Amer. J. Sci.* **262**, 735-752.

STEPHEN, J., SMITH, B.J., MARSHALL, D.C. & WITTAM, E.M. (1975): Applications of semiconductor backscattered electron detector in a scanning electron microscope. *J. Phys. E* **8**, 607-617.

STICKLER, R., HUGHES, C.W. & BOOKER, G.R. (1971): Application of the selected area – electron channelling pattern method to deformation studies. *Proc. Seventh Ann. Scanning Electron Microscopy Symp.* I, 473-483.

STOTT, D.E., WISE, M.L.H. & HUTCHINSON, W.B. (1975): A distortion-free map for use with electron channelling patterns. *J. Micros.* **105**, 305-307.

VAN ESSEN, C.G. (1971): Selected area diffraction in the SEM – towards one micron. *Proc. Twenty-fifth Ann. Meet. E.M.A.G., Cambridge,* Institute of Physics, London (abstr.).

———, SCHULSON, E.M. & DONAGHAY, R.H. (1971): The generation and identification of SEM channelling patterns from 10 μm selected areas. *J. Mat. Sci.* **6**, 213-217.

——— & VERHOEVEN, J.D. (1974): Rotation between micrographs from the scanning electron microscope and electron channelling patterns. *J. Phys. E* **7**, 768-770.

VENABLES, J.A. & HARLAND, C.J. (1973): Electron back-scattering patterns — a new crystallographic technique for use in the SEM. *In* Scanning Electron Microscopy: Systems and Applications. Institute of Physics, London.

WILLIAMS, R.O. (1968): The representation of the textures of rolled copper, brass and aluminium by biaxial pole figures. *Trans. Metall. Soc. A.I.M.E.* **242**, 105-115.

WOLF, E.D. & EVERHART, T.E. (1969): Annular diode detector for high angular resolution pseudo-Kikuchi patterns. *Proc. Second Ann. Scanning Electron Microscopy Symp.* I, 43-44 (abstr.).

YOUNG, C.T. & LYTTON, J.L. (1972): Computer generation and identification of Kikuchi projections. *J. Appl. Phys.* **43**, 1408-1417.

——— & ——— (1977): Computer generation and identification of divergent beam diffraction phenomena. *Int. Conf. Computer Simulation for Materials Application; Nucl. Metall.* **20**, 1244-1253.

Received March 1981, revised manuscript accepted September 1981.